JOURNAL OF MATERIALS SCIENCE **36** (2001) 1481–1486

Synthesis of $La_{1-x}Pb_xMnO_3$ colossal magnetoresistive ceramics from co-precipitated oxalate precursors

E. VLADIMIROVA, V. VASSILIEV
Institute of Solid State Chemistry, Ural Division of the Russian Academy of Sciences, 620219, Ekaterinburg, GSP-170, Russian Federation

A. NOSSOV
Institute of Metal Physics, Ural Division of the Russian Academy of Sciences, 620219, Ekaterinburg, GSP-170, Russian Federation
E-mail: nossov@imp.uran.ru

The precursors of $La_{1-x}Pb_xMnO_3$ manganite colossal magnetoresistive ceramics were prepared by co-precipitation process via the oxalate route using oxides as the starting materials. The mathematical model of the solution was developed and the conditions of the complete co-precipitation of all cations existing in the solution as insoluble oxalates were determined. $La_{1-x}Pb_xMnO_3$ manganites were synthesized by high-temperature thermal treatment of the precursors. It was demonstrated that the two-stage annealing procedure: 12 hours at 800°C in air and 12 hours at 950°C in flowing O_2 permits to synthesize compositions with the required stoichiometry exhibiting colossal magnetoresistive properties. © *2001 Kluwer Academic Publishers*

1. Introduction

The discovery of the "colossal" (up till 127000% [1]) magnetoresistance (CMR) in the doped manganites had renewed the interest to this class of complex oxide materials of general formula $Ln_{1-x}M_xMnO_3$, where Ln = La, Nb, Pr and M = Ca, Ba, Sr, Pb [2, 3]. Pb-containing manganites, as well as Ca and Sr ones, have the distorted perovskite ABO_3 structure with the phombohedral unit cell [4]. The parent $LaMnO_3$ compound is an antiferromagnetic insulator. Substitution of A-site trivalent cation by the divalent one leads to the mixed valence of Mn ions that in the case of La manganites can be described as $La_{1-x}M_xMn^{3+}_{1-y}Mn^{4+}_yO_3$. Compositional variations of resistivity, magnetic and magnetotransport properties of Pb-doped manganites can be interpreted in the framework of the double exchange model [5] considering the electron transfer with spin memory between the Mn ions of different valence as the basic physical mechanism responsible for conductivity. Large negative magnetoresistance $MR(H, T)$ is observed in the vicinity of the ferromagnetic ordering temperature (T_C) and is due to the suppression of spin fluctuations by the magnetic field. The conductivity type also changes from metallic-like in the ferromagnetic low temperature region to the semiconductor-like in the paramagnetic high temperature region where MR drastically drops with temperature. In a case of polycrystalline sintered materials large magnetoresistance can be observed at low-temperatures as a result of spin-polarized electron tunneling at the grain boundaries.

In the family of CMR manganites, the materials doped with Pb are of special interest, because they have rather high T_C and the significant magnetoresistance is observed at room temperature. That can be important for possible device applications. We define here magnetoresistance as $MR(H, T) = (\rho(H, T)\text{-}\rho(0, T))/\rho(0, T)^*100\%$, where $\rho(0, T)$ and $\rho(H, T)$ are the resistivity values in zero field and under the applied magnetic field H at temperature T. For $La_{0,69}\ Pb_{0,31}MnO_3$ [6] and $La_{0,60}\ Pb_{0,40}MnO_3$ [7] single crystals the reported values are MR (10 kOe, 325 K)∼18% and MR (60 kOe, 315 K) ∼ 65%, respectively. Historically [6], the first CMR manganite single crystals were obtained in the La-Pb system and since that time a great number of publications were devoted to the studies of magnetic and transport properties of single crystalline and bulk polycrystalline sintered samples. The available experimental T_C values at compiled at Fig. 1. The most numerous studies were carried out for the $X = 0.4$ composition. For single crystals the difference between T_C values is 14 K (compare [6] and [8]) while for polycrystalline samples it is slightly higher and is 20 K ([9] and [10]). The general tendency is the gradual increase of T_C with X which is more pronounced for the single crystalline samples. It should be pointed out that T_C values for polycrystalline samples with $X = 0.26$ [10] and 0.33 [11] are lower 300 K. We can mark much large spread of T_C values for polycrystalline samples as compared to the single crystals of the same composition, that can indicate the peculiarities of

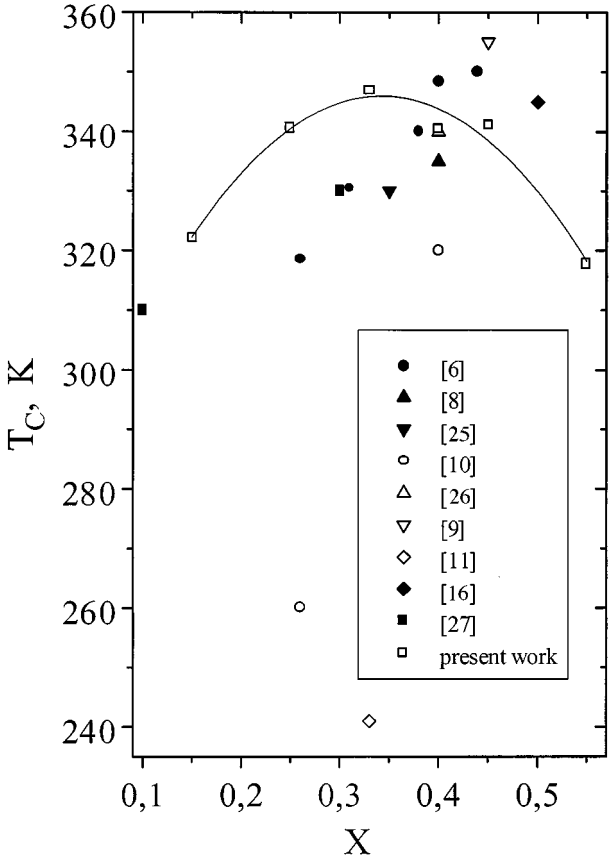

Figure 1 Comparison of the Curie temperatures for $La_{1-x}Pb_xMnO_3$ manganites. Opened symbols-polycrystalline samples, filled symbols - single crystals. Solid line – results of the present work.

synthesis and annealing of La-Pb manganites. At the same time, the polycrystalline manganites are of special interest as soon as their synthesis procedure is much faster and easier as compared to the single crystals, and they are widely used for thin film preparation as the targets for laser ablation and magnetron sputtering.

The traditional synthesis of manganites by solid state or ceramic route involves the high-temperature (1100–1300°C) annealing of the carbonates or oxides mixtures in a controlled atmosphere. Meanwhile, it is well known that the lead oxide starts to melt at 890°C and evaporates as Pb_2O_2 and Pb_4O_4 [4, 12] upon further increase of temperature. For the temperature range 887–1151 K the vapor pressure temperature dependence for PbO can be expressed as $\log P(Pa) = 13{,}71\text{-}13{,}86 \times 10^3/T(K)$ [12]. That's why it is rather difficult to obtain the La-Pb samples of the required stoichiometry by the traditional ceramic route.

In this paper we describe the co-precipitation technique for the precursor synthesis and thermal treatment procedure, resulting in preparation of CMR $La_{1-x}Pb_xMnO_3$ manganites of the predetermined stoichiometry.

2. Experimental

Bulk polycrystalline $La_{1-x}Pb_xMnO_3$ samples ($0 < X < 1$) were synthesized by chemical treatment of the precursors. It is known that this method permits to prepare the products with better magnetic and phase homogeneity as compared to the traditional ceramic "shake and bake" technology [13]. Thermal processing of the precursors permits to lower the synthesis temperature to 950°C and thereby circumvent compositional variations of the final product. Sintered densities were determined by the Archimedes method using ethanol. X-ray diffraction analysis was performed using Cu K_α radiation (STADI-P, STOE). After sintering the samples were examined with optical techniques and scanning electron microscopy.

The magnetic and transport properties of the $La_{1-x}Pb_xMnO_3$ manganites were studied for the samples with $X = 0{,}15$; 0,25; 0,33; 0,40; 0,45 and 0,55. The magnetization curves were measured for the temperature range 5–400 K with maximum applied magnetic field 80 kOe. Curie temperatures were determined from Arrott-Belov plots. Magnetoresistance was measured by the standard four-probe technique in the temperature range 5–300 K and applied magnetic field till 50 kOe with current parallel to the magnetic field.

3. Results and discussion

Various wet chemical methods of precursor synthesis are described in the literature [4, 14, 15] utilizing the co-precipitation of the citrates, carbonates and the salts of complex organic acids. We had developed rather simple method of precursor synthesis by co-precipitation of the insoluble metal oxalates.

The necessary condition for preservation of the desired stoichiometry is the complete transfer of the metal ions into the precipitating phase. The mathematical model of the solution was developed considering the interaction of Mn, La and Pb nitrates with oxalic acid as a precipitator. Different processes can take place in this solution:

- formation of the insoluble oxalates according to the reaction

$$KM^{n+} + mC_2O_4^{2-} = [M_K(C_2O_4)_m]^{kn-2m} \qquad \beta_{mk} \quad (1)$$

- oxalic acid protoionisation

$$C_2O_4^{2-} + H^+ = HC_2O_4^- \qquad \beta_1 \quad (2)$$

$$C_2O_4^{2-} + 2H^+ = H_2C_2O_4 \qquad \beta_2 \quad (3)$$

- formation of metal hydrocomplexes

$$iM^{n+} + jOH^- = [M_iOH_j]^{i-j} \qquad \beta_i \quad (4)$$

where β_j are the corresponding equilibrium constants. The β_j values were calculated using the reference data according to the equation

$$\Delta G = -RT\ln\beta_j, \quad (5)$$

where ΔG- variation of Gibbs energy for the corresponding reaction, $R = 8.31$ J/molK- universal gas constant, T- temperature. The equations of the reactions and the corresponding equilibrium constants are listed

TABLE I Formation logarithms for corresponding reactions

Equation	$\lg\beta_{ij}$							
$C_2O_4^{2-} + iH^+ = H_iC_2O_4^{2-i}$	i	1	2					
	$\lg\beta_i$	1.2	4.3					
$iMn^{2+} + jOH^- = Mn_i(OH)_j^{2i-j}$	ij	11	12	13	14	23		
	$\lg\beta_{ij}$	3.38	5.72	8.40	7.57	16.2		
$iLa^{3+} + jOH^- = La_i(OH)_j^{3i-j}$	ij	11	12	13	14	59		
	$\lg\beta_{ij}$	5.4	10.7	16.0	18.9	54.4		
$iPb^{2+} + jOH^- = Pb_i(OH)_j^{2i-j}$	ij	11	12	13	14	34	44	68
	$\lg\beta_{ij}$	6.1	10.9	13.7	16.5	32.0	35.0	68.2
$Mn^{2+} + C_2O_4^{2-} = MnC_2O_4$	$\lg\beta$	7.2						
$2La^{3+} + 3C_2O_4^{2-} = La_2(C_2O_4)_3$	$\lg\beta$	26.4						
$Pb^{2+} + C_2O_4^{2-} = PbC_2O_4$	$\lg\beta$	6.54						

TABLE II The fraction of precipitated metal (mass %) for $La_{0.67}Pb_{0.33}MnO_3$

	pH											
Cation	1	2	3	4	5	6	7	8	9	10	11	12
La^{3+}	99.8	99.9	100	100	100	100	100	100	100	100	99.7	97.8
Mn^{2+}		98.5	99.6	99.7	99.7	99.7	99.7	99.4	99.0	94.6	70.0	0
Pb^{2+}	99.5	99.8	100	100	100	100	100	99.8	99.3	95.6	80.6	0

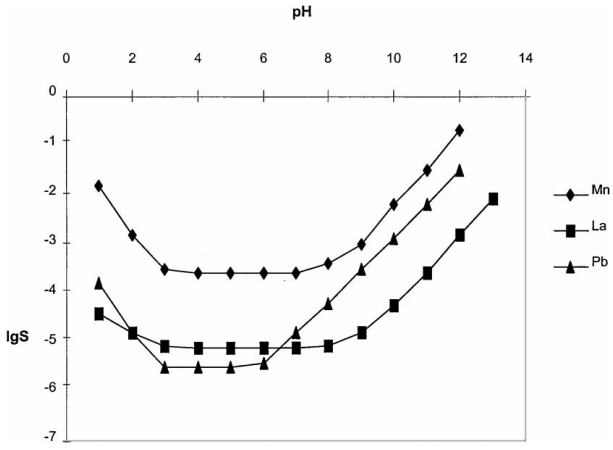

Figure 2 pH dependence of metal oxalates solubility.

in Table I. Concentration of the ions in the solution and the precipitated metal fraction were determined by solving the system of equations. Using the pH dependence of the oxalates solubility, the limits of the pH region were determined within which all the metals contained in the solution are completely precipitated. The dependence of metal oxalate solubility on the pH of the solution is presented at Fig. 2. As one can see from Fig. 2 the region of minimum solubility is rather wide and is limited by pH = 3–6. It is possible to calculate the fraction of the sedimented metal in order to be certain that precipitation of metals in the selected pH region will result in preparation of compositions with the required stoichiometry. In order to prepare the sample with $X = 0.33$, the nitrates concentration in the solution must be $La(NO_3)_3 = 0.066$; $Mn(NO_3)_2 = 0.1$; $Pb(NO_3)_2 = 0.033$ mol/l. The pH dependence of the sedimented metal percentage content was calculated using these given concentrations and oxalates solubility. The results are presented in Table II. According to these data it is clear that for the selected pH region all the metals are transferred into the precipitated phase practically completely. The fraction of metal remaining in the solution is so small, that it can not alter the stoichiometry of the final product.

$La_{1-x}Pb_xMnO_3$ precursors were prepared according to the following route. The starting oxides PbO, Mn_2O_3, La_2O_3 were dissolved in the nitric acid in the presence of H_2O_2 to reduce the manganese to Mn^{2+}. Fixed pH = 4 was kept by addition of the appropriate quantities of HNO_3 or NH_4OH. The solution of the oxalic acid was then added till complete precipitation of the oxalates. The sedimented precipitate was rinsed in distilled water, separated by decantation technique, and dried in air at room temperature. Thus obtained precursors were precalcinated at 800°C in air for 12 hours, then pelletized, and further annealed at 950°C in flowing O_2 for another 12 hours. The existence of the continuous set of solid solutions with perovskite structure for $La_{1-x}Pb_xMnO_3$ manganites within the composition range $0 < X < 0.4$ was confirmed by X-ray structural analysis. Lead and manganese concentrations, as well as Mn^{3+}/Mn^{4+} ratio, were determined by potentiometric titration in order to verify the stoichiometry of the samples. The results are listed in Table III. With reference to Table III, one can see that thus defined concentration of Pb^{2+} is in good agreement with the theoretical values.

TABLE III The results of $La_{1-x}Pb_xMnO_3$ quantitative analysis

	Pb content (mass %)		Total Mn content (mass %)			
X	theor.	Exp.	theor.	exp.	Mn^{3+}	Mn^{4+}
0,15	12,3	12,2	21,8	22,5	6.93	15.6
0,25	20,0	20,0	21,2	21,2	4.56	16.6
0,33	25,86	26,1	20,8	21,3	4.53	16.8
0,40	30,76	30,3	20,45	22,0	4.5	17.5
0,45	34,18	34,6	20,18	21,5	5.6	15.9
0,55	40,73	40,0	19,7	21,0	8.26	12.8

Hence, utilization of the precursors obtained by the co-precipitation technique, permits to lower the synthesis temperature and to obtain the La-Pb manganites of the predetermined stoichiometry.

While the compositions with $X \leq 0.4$ were found to be the single-phase perovskites, the additional $Pb_3Mn_6O_{13}$ phase was found in the samples with $X > 0.4$. Its quantities for $La_{0.55}Pb_{0.45}MnO_3$ and $La_{0.45}Pb_{0.55}MnO_3$ compositions were found to be 8 and 25% respectively. The presence of the additional $Pb_3Mn_6O_{13}$ phase (~13%) was also reported in [16] for the $La_{0.50}Pb_{0.50}MnO_3$ composition. From our data we can estimate the quantity of the additional phase for the $X = 0.5$ composition. The obtained result of 16.5% is in satisfactory agreement with [16]. The difference between the exact values can be ascribed to various preparation routes (traditional ceramic technology was used in [16]), sintering atmosphere (air in [16] and oxygen in our case) and duration (24 hours in [16] and 12 hours in our case). It was demonstrated earlier [17] that magnetic and transport properties of doped manganites strongly depend on the annealing duration.

The ratio of the sintered density to the theoretical X-ray density had varied regularily with Pb doping level from 0.71 to 0.63 for $0.15 \leq X \leq 0.40$. Similar trends in the sintering behavior of doped manganites with varying deficiency of the A-site cation ratio of the ideal ABO_3 perovskite structure were observed in [18] for Sr-doped manganites.

The grain size of the samples under consideration was found to be of the order of ~3 μm and did not vary substantially from sample to sample. Large low-field grain boundary magnetoresistance (LFMR) due to the spin-polarized carriers tunneling (or scattering) at the interfaces between the individual grains was observed at low temperatures. To quantify this contribution of grain boundary properties into the processes of the electric current transport, the high field regions of MR(H, 5 K) curves were back-extrapolated to find the zero field intercept. As it was shown in [19] to the first approximation LFMR~ $-J^*P^*\Delta m^2/T$ where J is the intergrain exchange constant, P is the electron polarization, T is the temperature, and $\Delta m^2 = m^2(H, T) - m^2(0, T)$ is the variation of normalized magnetization under the influence of the applied magnetic field. For the fixed temperature LFMR~ $-P$. Fig. 3 presents the comparison of doping dependencies for LFMR and saturation magnetization at M_{sat}(5 K). Clear correlation between these data reflects variation of the spin polarization of carriers at Fermi level with doping and the fact that the mechanism of spin-polarized carriers tunneling gives the major contribution to LFMR [20].

Compositional dependence of T_C, saturation magnetization at 5 K (M_{sat}) and ρ(0, 300 K) are presented at Fig. 4. Pronounced correlation between the M_{sat}(5 K) and T_C is observed. The highest T_C corresponds to the most perfect alignment of manganese ions magnetic moments. Similar relation is observed between the magnetic and transport properties: maximums of $M_{sat}(X)$ and $T_C(X)$ curves are corresponding to the minimum of $\rho(X)$. According to the double exchange model [5] the probability t_{ij} of electron transfer along the Mn-O-Mn chain depends on the angle θ_{ij} between

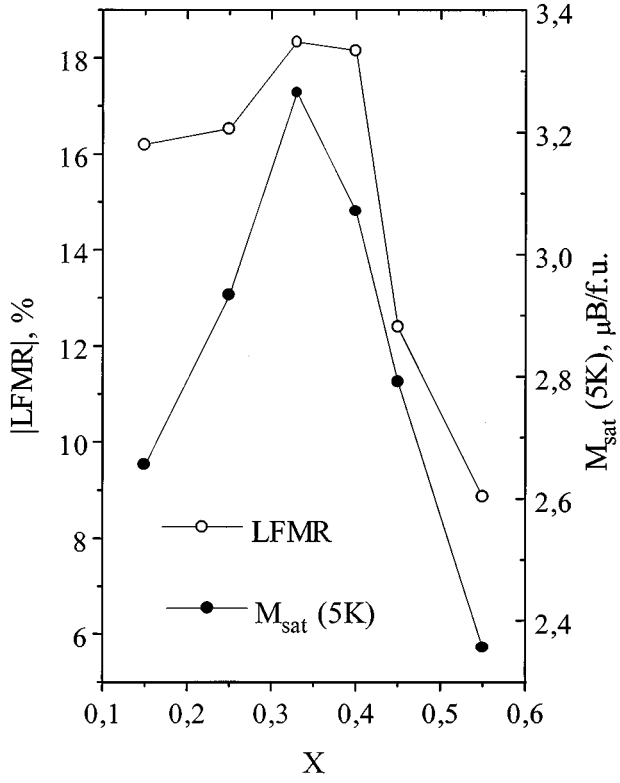

Figure 3 Comparison of doping variation of the low-field magnetoresistance (see definition in the text) and saturation magnetization at M_{sat}(5 K).

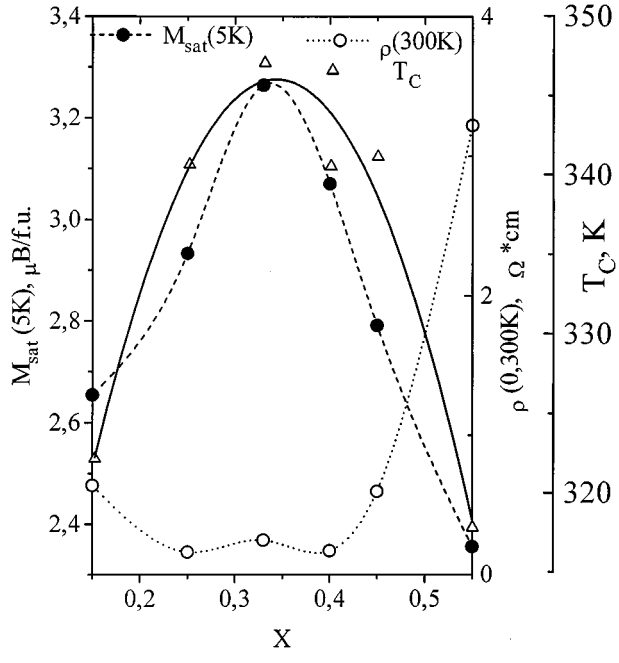

Figure 4 Compositional dependence of Curie temperature (T_C); saturation magnetization at 5 K (M_{sat}) and resistivity at 300 K (ρ(0, 300 K)) for $La_{1-x}Pb_xMnO_3$ manganites.

the adjacent spins of Mn ions as $t_{ij} \sim \cos\theta_{ij}$ and is maximum for the ferromagnetic type of ordering for which θ_{ij} is minimal.

Temperature variation of the spontaneous magnetization of the samples under consideration is presented at Fig. 5. One can see that the sharpness of the curves is the highest for compositions with $X = 0.33$ and 0.4. The value of M_{sat}(5 K) for $X = 0.33$ is the highest and corresponds to the most perfect ferromagnetic type of

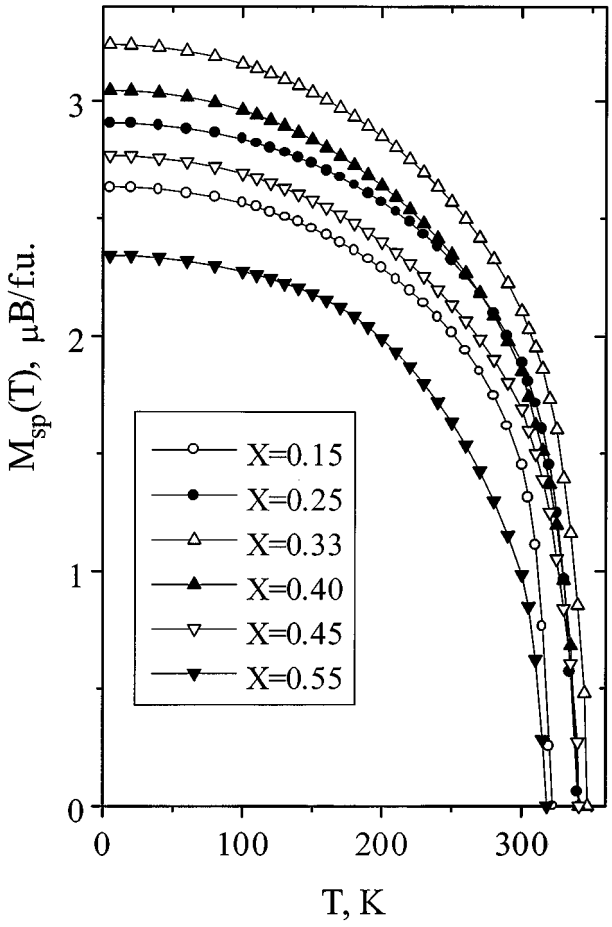

Figure 5 Temperature variation of the spontaneous magnetization for $La_{1-x}Pb_xMnO_3$ manganites.

magnetic ordering for the samples under consideration. Decrease of M_{sat}(5 K) values with deviation of the dopant concentration from 0.33 may be due to the appearance of the other types of magnetic ordering, for example some canted structures, or even the magnetic inhomogeneity. It is difficult to make any conclusion about the type of these structures only from our magnetization data. Different magnetic phases were found in doped manganites [21]: ferromagnetic and paramagnetic insulating, ferromagnetic and paramagnetic metallic, various canted phases. The exact stricture is defined by complex interplay between the magnetic, structural and spin degrees of freedom. Composition with $X = 0.15$ is of the particular interest. This doping level is very close to the theoretical value of percolation threshold $X \cong 0.16$ [22] when the divalent doping ions are starting to form the infinitive claster, though the exact value of the percolation threshold depends on the type of the crystal lattice and microscopic correlation mechanisms. Doping of manganites by divalent cations leads to introduction of carriers (holes) into the system and appearance of ferromagnetic interaction due to the double-exchange mechanism because the hole transfer with spin memory along the same Mn-O-Mn chain is responsible for both magnetism and conductivity. In the vicinity or percolation threshold the ferromagnetic type of ordering can exist within the microscopic cluster, but it may be no percolation between the clusters. Then different properties can be observed. The $La_{0.85}Sr_{0.15}MnO_3$ composition was found to be the ferromagnetic insulator [21]. At low doping levels, for example for $La_{0.90}Sr_{0.10}MnO_3$ composition, the experimental results can be interpreted only within the framework of the mixed ferromagnetic - antiferromagnetic ground state model [23] assuming the presence of ferromagnetic clusters in the non-ferromagnetic matrix (magnetic phase separation). In our case the M_{sat}(5 K) value for $La_{0.85}Pb_{0.15}MnO_3$ composition is only 2.6 Bohr magnetons and the $M_{sat}(T)$ curve goes much lower than that for compositions with higher doping levels. Below Curie temperature the sample is in the ferromagnetic metallic state. The discrepancy of the observed and theoretical values of saturation magnetization can be ascribed to the presence of some additional magnetic structure (some canted structure or the magnetic inhomogeneity) though the additional experimental studies are required to clarify this point.

The series of MR(H, 300 K) curves are presented at Fig. 6. For such high temperatures the LFMR contribution is almost vanishing. Almost linear decrease of resistivity is observed reflecting the suppression of the spin disorder by the external magnetic field as it was also observed in [20, 24]. Compositional dependence of magnetoresistance for the maximum applied magnetic field 50 kOe is shown at the inset of Fig. 6. Rather slight variations of magnetoresistance are observed for $X > 0.2$. As soon as the MR(H, T) dependence has the peak in the vicinity of the ferromagnetic ordering temperature, the local maximum magnetoresistance value corresponding to $X = 0.15$ is due to the smallest difference between T_C and the temperature of measurement (300 K). Since the samples with $X > 0.4$ are not single phase ones, it is worthwhile to analyze the influence

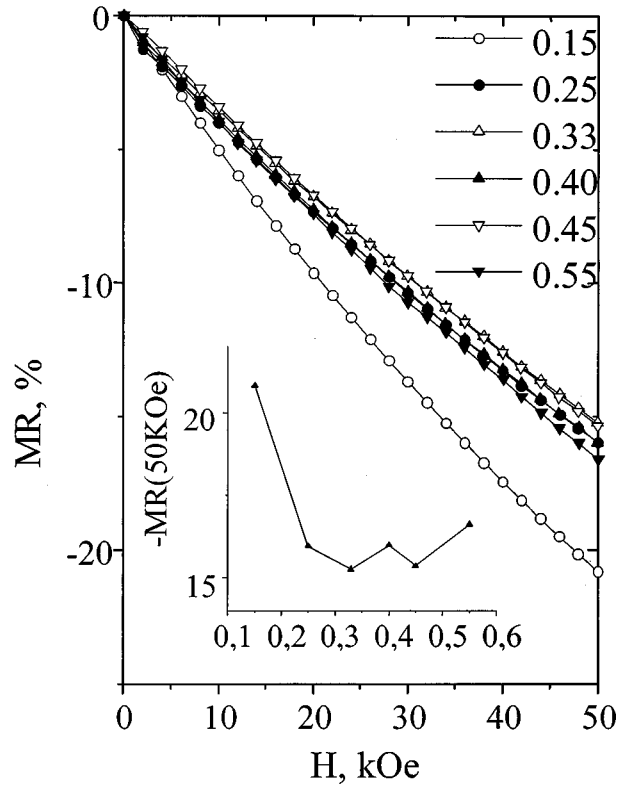

Figure 6 Magnetic field dependence of magnetoresistance at 300 K. Inset: Compositional dependence of MR(50 kOe, 300 K).

of the additional phase on the physical properties inasmuch as its content increases with X. From the data presented at Fig. 4 it is clear that the most pronounced relative increase is observed for $\rho(0, 300\ \mathrm{K})$ as soon as the additional phase is probably low conducting. The relative decrease of the magnetic parameters (T_C and $M_{sat}(5\ \mathrm{K})$) as well as of the magnetoresistance value is much smaller.

The Curie temperature values for our samples are compared to the available literature data and are also presented at Fig.1. Reasonable consistency is observed for $X > 0.3$. For the most studied $La_{0.60}Pb_{0.40}MnO_3$ composition, the T_C value of our bulk sintered polycrystalline sample coincides with that of the single crystal [8]. For $X < 0.3$ the T_C values for all our samples are exceeding 300 K being much closer to the data corresponding to single crystals than for compositions synthesized by the traditional ceramic route [10, 11]. Considering Pb- and Sr-doping of lanthanum manganites it is interesting to note that the decrease of T_C for low doping levels is much less pronounced for Pb-doped system. Comparing compositions with the same doping level $X = 0.15$ one can see that $T_C = 240$ K for Sr doping, but $T_C = 322$ K for Pb doping. That makes Pb-doped manganites more promising for possible practical applications.

In summary, we have defined the conditions of CMR $La_{1-x}Pb_xMnO_3$ manganite synthesis via co-precipitation route. Utilization of the precursors, obtained by the described technique, permits to lower the sintering temperature and preserve the stoichiometry of the final product. For the samples of the $0.15 < X < 0.55$ composition range obtained by this technique the smooth variation of the magnetic and magnetotransport properties is observed with strong correlation between ferromagnetic ordering type and resistivity as a result of double exchange interaction. This correlation is most pronounced for $X = 0.3$ doping level.

References

1. E. NAGAEV, *Uspekhi Fizicheskih Nauk* **166** (1996) 833 (in Russian, translated in English as Soviet Phys.:Uspekhi).
2. P. RADAELLY, M. MAREZIO, H. HWANG and S.CHEONG, *Phys. Rev. Lett.* **75** (1995) 4488.
3. S. JIN, H. O'BRYAN, T.TIEFEL, M. MCCORMAC and W. RHODES, *Appl. Phys. Lett.* **66** (1995) 382.
4. "Gmelin Handbuch der anorganischen Chemie. Mangan.," C3 (Springer-Verlag, 1975).
5. P.-G. DE GENNES, *Phys. Rev.* **118** (1960) 141.
6. C. SEARLE and S. WANG, *Can. J. Phys.* **48** (1970) 2023.
7. X. JIA, L. LU, K. KHAZENI, V. CRESPI, A. ZETTL and M. COHEN, *Physical Review B* **52** (1995) 9147.
8. E. SVIRINA, L. SHLYAKHINA and M. LUKINA, *Sov. Phys. Solid State* **24** (1982) 1947.
9. I. TROYANCHUK, L. BALYKO and G. BYCHKOV, *ibid.* **31** (1989) 1830.
10. M. SAHANA, K. SATYALAKSHMI, M. HEDGE, V. PRASAD and S. SUBRAMANYAM, *Mater. Res. Bull.* **32** (1997) 831.
11. C. BOOTH, F. BRIDGES, G. SNYDER and T. GEBALLE, *Phys. Rev. B* **54** (1996) 15606.
12. N. POLYANSKII, *Lead*, "Nauka," 1976 (in Russian).
13. V. VASSILIEV, A. IWAKIN and A. FOTIEV, *Russ J. Inorg. Chem.* **39** (1994) 1.
14. J. MITCHELL, D. ARGYRIOU, C. POTTER, D. HINKS, J. JORGENSEN and S. BADER, *American Physical S.* **54** (1996) 6172.
15. J. ALONSO, M. MARTINEZ-LOPE and M. CASIAS, *Eur. J. Solid State Inorg. Chem.* **33** (1996) 331.
16. A. SHAMES, E. ROZENBERG, G. GORODETSKY, J. PELLEG and B. CHANDHURI, *Solid State Commun.* **107** (1998) 91.
17. J. PIERRE, A. NOSSOV, V. VASSILIEV and V. USTINOV, *J. Phys.: Cond. Matter* **8** (1996) 8513.
18. J. STEVENSON, P. HALLMAN, T. ARMSTRONG and L. CHICK, *J. Amer. Ceram. Soc.* **78** (1995) 507.
19. H. Y. HWANG, S.-W. CHEONG, N. P. ONG and B. BATLOGG, *Phys. Rev. Lett.* **77** (1996) 2041.
20. S. LEE, H. HWANG, B. SHRAIMAN, W. RATCHIFF and S. CHEONG, *ibid.* **82** (1999) 4508.
21. A. URUSHIBARA, Y. MORITOMO, T. ARIMA, A. ASAMITSU, G. KIDO and Y. TOKURA, *Phys. Rev. B* **51** (1995) 14103.
22. J. M. ZIMAN, "Models of Disorder" (Cambridge: Cambridge University Press), 1979.
23. A. V. KOROLYOV, V. YE. ARKHIPOV, V. S. GAVIKO, YA. MUKOVSKII, A. A. ARSENOV, T. P. LAPINA, S. D. BADER, J. S. JIANG and V. I. NIZHANKOVSKII, *JMMM* **213** (2000) 63.
24. Ll. BALCELLS, J. FONTCUBERTA, B. MARTINEZ and X. OBRADOS, *Phys. Rev. B* **58** (1998) R14697.
25. R. JANES and R. BODNAR, *J. Appl. Phys.* **42** (1971) 1500.
26. I. TROYANCHUK, L. BALYKO and G. BYCHKOV, *Sov. Phys. Solid State* **31** (1989) 716.
27. R. MAHENDIRAN, R. MAHESH, A. RAYCHAUDHURI and C. RAO, *J. Phys. D: Appl. Phys.* **28** (1995) 1743.

Received 12 August 1999
and accepted 3 August 2000